

An Experimental and Numerical Investigation of Fluid Flow and Heat Transfer in Different Micro-channels

Dr. A.P. Singh¹, Mohd. Ghufuran Ali Siddiqui²

¹Associate Professor, Department of Physics Hindu College Moradabad, Uttar Pradesh, India

²Research Scholar, Department of Physics, IFTM University Moradabad, Uttar Pradesh, India

ABSTRACT

We expanded the continuum momentum and energy equations for laminar forced convection in two-dimensional V-Shaped micro-channels and nano-channels under hydrodynamically and thermally fully developed conditions with the first-order velocity slip and temperature jump boundary conditions at the channel walls. Closed form solutions are obtained for the fluid friction and Nusselt numbers in the slip-flow regime. DI water, Methanol, Nano are use as the working fluid and flow through micro-channels with different hydraulic diameters ranging from 57–267 μm in the experiments we examined the experimental results of flow characteristics & check behavior of the laminar regime when $\text{Re} = 50\text{--}850$. The Reynolds number at transition from laminar to turbulent flow is considered. Attention is paid to comparison between predictions of the conventional theory and experimental data, obtained during the last decade, as well as to discussion of possible sources of unexpected effects which were revealed by a number of previous investigations. Experimental results in heat transfer indicted that forced convection in micro channel heat sink exhibited excellent cooling performance, especially in the phase change regime. It will be applied as heat removal and temperature control devices in high power electronic components. When the critical nucleate heat flux condition appeared, flow mechanism changed into fully developed nucleate boiling and accompanied with wall temperature decreased rapidly and pressure drop increased sharply. Experimental results also indicated that the critical bubble size of methanol was between 54–85 μm .

Keywords: Micro Channels, Fluid Mechanics, Heat Transfer Techniques, Hydraulic Diameters.

I. INTRODUCTION

In contrast to external flow, the internal flow is one for which the fluid is confined by a surface. Hence the boundary layer develops and eventually fills the channel. The internal flow configuration represents a convenient geometry for heating and cooling fluids used in chemical processing, environmental control, and energy conversion technologies. In the last few decades, owing to the rapid developments in micro-electronics and biotechnologies, the applied research in micro-coolers, micro-biochips, micro-reactors, and micro-fuel cells have been expanding at a tremendous pace. Among these micro-fluidic systems, micro

channels have been identified to be one of the essential elements to transport fluid within a miniature area. In addition to connecting different chemical chambers, micro channels are also used for reactant delivery, physical particle separation, fluidic control, chemical mixing, and computer chips cooling. The microchannel heat sink under the Micro-Electro-Mechanical Systems (MEMS) has first been illustrated in 1981 [1]. Their theoretical analyses and experimental tests were conducted to investigate the characteristics of heat transfer in the microchannel heat sink. Up to 790 W/cm^2 of heat flux was

implemented to Very Large Scale Integration (VLSI) with high power density.

Zhimin and Kok-Fah [2] have also integrated the optimum design considering the laminar and turbulent flows in the channels to construct a thermal resistance model for simulating the fluid dynamics and heat transfer characteristics in the microchannel heat sinks. Many researchers [3,4] indicated that the prediction of heat transfer in the micro devices varied from that in macro devices.

Pfahler et al. [5] and Choi et al. [6] proposed the experimental results to show the different fluid and heat characteristics in the micro and macro channels as well as the tubes. Their works definitely provided the valuable conception in the heat and fluid properties of the single-phase flows.

Mohiuddin-Mala and Li [7] experimentally investigated the fluid characteristics for the silica and stainless tubes of hydraulic diameters ranging from 50 to 254 μm . Qu Weilin et al. [8] have also studied the behaviors for trapezoid silicon microchannels of a hydraulic diameter from 51 to 169 μm . Their results have contradicted the conventional macochannels with much effective heat.

Many researchers [9–15] have focused on the heat behavior during phase transformation. It has been observed that no bubbles from nucleate boiling occurred in microchannels even with the high heat flux. The evidence that the channel size is a critical parameter to the phase change is a major approach to the future research of two-phase fluid.

Peng and Wang [16–18] have then analyzed the boiling characteristics and heat phenomenon, especially the formulation and growth of the bubbles, to obtain the effects of the channel. Their results showed that it is almost impossible to have nucleate boiling in the microchannels. However,

Linan Jiang et al. [19] have conducted the in-situ measurement to explore the two-phase behaviours of nitrogen in silicon micro channels of hydraulic diameter from 40 to 80 μm . It was shown that no plateau but steeply rising of the wall temperature in boiling curve when reaching the critical heat flux.

[4]Naphon P. Heat transfer characteristics and pressure drop in channel with V corrugated upper and lower plates. *Energy Convers Manag*2007;48: 1516–24.

[8] Naphon P, Kornkumjayrit K. Numerical analysis on the fluid flow and heat transfer in the channel with V-shaped wavy lower plate. *Intl Commun Heat Mass Transf*2008;35:839–43.

This paper not only proposes the micro channels with anisotropic etching on the (100) silicon wafer, but also examine the process of fluid flow and heat transfer, especially the mechanism of bubble nucleation. Through the fluid behaviours and the thermal phenomenon discussed in this study, the demand for future heat removal among the electronic components is concretely solvable.

Definition	The range of channel dimension
Conventional channels	$D_c > 3 \text{ mm}$
Mini-channels	$3 \text{ mm} \geq D_c > 200 \mu\text{m}$
Micro-channels	$200 \mu\text{m} \geq D_c > 10 \mu\text{m}$
Transitional Micro-channels	$10 \mu\text{m} \geq D_c > 1 \mu\text{m}$
Transitional Nano-channels	$1 \mu\text{m} \geq D_c > 0.1 \mu\text{m}$
Nano-channels	$D_c \leq 0.1 \mu\text{m}$

II. METHODOLOGY AND EXPERIMENTAL MEASUREMENT

As the field of micro-fluidic systems continues to grow, it is becoming increasingly important to understand the mechanisms and fundamental differences involved in micro-scale fluid flow. To study the thermal and hydrodynamic characteristics of fluid flow in micro-channels, this work used experimental measure and numerical to investigate

the behavior of flow and temperature fields in micro channels. To carry out the experiments of the flow in micro channels, first and foremost, a fluid flowing and measurement system, together with micro channel structures has been properly designed and built up as shown in figure 2 & 3.

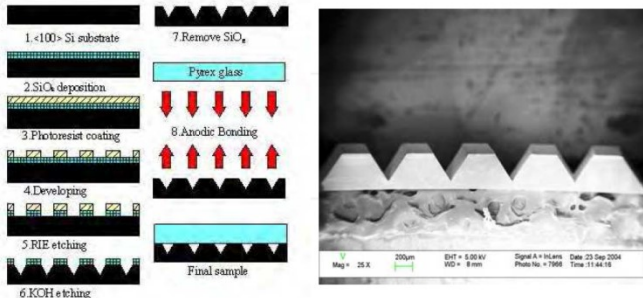


Figure 1. a) Fabrication of silicon micro channels (b) V-shaped Micro channel

2.1 Test Section

The experimental system was divided into three parts – the test section, the Fluid and Heat driving system, and the Dynamic data Acquisition section. The experimental system heating resistance a thermal source in electronics device and methanol, DI water (de-ionized water) is used as a working fluid to evaluate heat transfer in V-shape and other geometrical micro channel. .

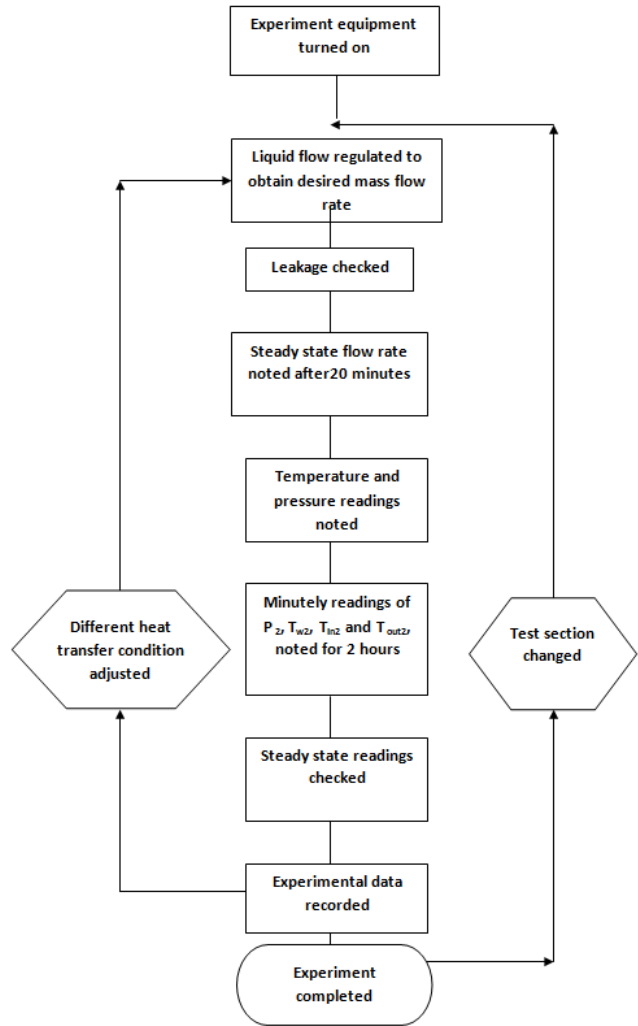


Figure 2. Experimental Steps

Table 1. Specification fo the sink

Chip name	Width (µm)	Depth (µm)	Hydraulic diameter (µm)	Number of channel
	W _c	H _c		
Chip 1	350	220	175	10
Chip 2	250	100	160	11
Chip 3	200	150	124	18
Chip 4	170	140	98	20
Chip 5	150	95	83	25

The detailed experimental drawing, including liquid tank, liquid pump, 5 µm filter, flow meter, heat exchanger, is shown as Figure 3.

Table 2

Experimental Uncertainties	
Parameter	Uncertainty (%)
Flow rate	4.0
Pressure drop	3.0
Temperatures	1.5
Reynolds number	6.4
Friction factor	12.0

The experimentally-measured data were composed of pressure drop through the micro-channel, temperatures of DI water and substrate, and the mass flow rate. For the manufacture of microchannels, photolithographic processes are particularly utilized for silicon wafers, and these processes initiated in the electronic field are well developed. When a photolithography-based process is employed, the microchannels having a cross-section fixed by the orientation of the silicon crystal planes can be fabricated; for example, the micro channels etched in <57> or in <267> silicon by using a Methanol, DI water, Nano solution.

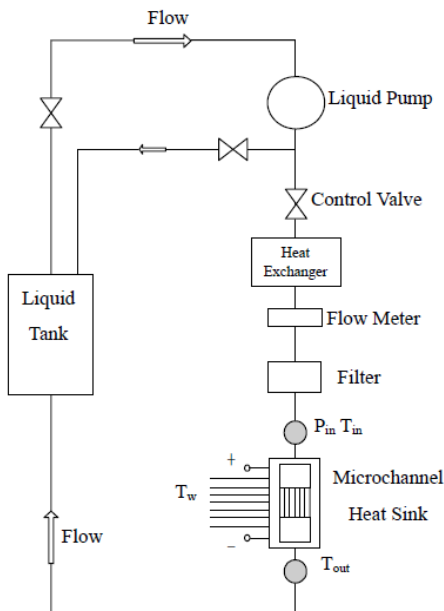


Figure 3. Experimental Layout

The working fluid remains at a constant temperature by the liquid tank and heat exchanger, and then pumped through the filter that prevents the

extraneous particles and air to the flow meter and microchannels. The thermo-couples and the pressure sensors are settled into both the inlet and outlet of the microchannel heat sink to the temperature as well as the pressure drop. The thermo-couples are also attached to the back of the micro channel heat sink for the measurement of the wall temperature. Under steady state, all data in each experiment can be obtained through the data acquisition system, and then transferred to the computer for computation.

2.2 Fluid and Heat Driving System

The theoretical and the experimental friction factor are expressed as:

$$f_{thy} = 64 / Re \dots\dots\dots(I)$$

$$f_{exp} = 2g_c \Delta P D_h / L \rho_f V_f^2 \dots\dots\dots(II)$$

$$\Delta P_{loss} = K \rho_f V_f^2 / 2g_c \dots\dots\dots(III)$$

length of microchannels $L = 15000 \mu m$

The friction factor of micro channels is computed by theoretically and experimentally with the help of Eq. (I) and Eq. (II) respectively. The experimental friction factor is build from the experimental measurement by, and then compared to the theoretical. On the measurement of pressure drop, the pressure cannot be in-situ measured by the sensor because of the micro scale of the channels. Therefore, the pressure measured should subtract the pressure loss (ΔP_{loss}) shown in Eq. (III), where K is the pressure loss coefficient. Thus, $K = 1.0$ for the inlet and $K = 0.5$ for the outlet [8] are also suggested in this study.

The heat flux is commonly stated as

$$q'' = rIV / LW \dots\dots\dots(IV)$$

Here, V and I denote the voltage and current delivered from the power supply, respectively. and, L and W present the overall channel length and channel width, respectively. The mended factor, r , in Eq. (IV) is applied to describe the sensible heat held in between the inlet and outlet.

2.3 Dynamic Data Acquisition Section

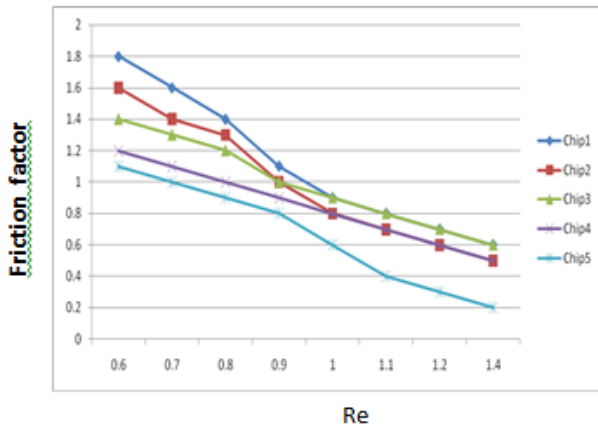


Figure 4. Relation between friction and Renold's numbers

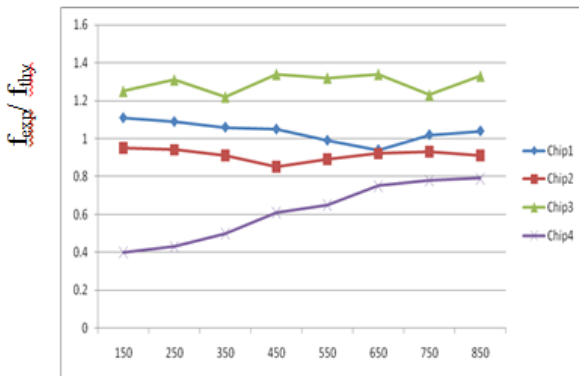


Figure 5. f_{exp}/f_{thy} and the Renold number

Table 4

f_{exp}/f_{thy}	Chip1	Chip2	Chip3	Chip4
150	1.11	0.95	1.25	0.4
250	1.09	0.94	1.31	0.43
350	1.06	0.91	1.22	0.5
450	1.05	0.85	1.34	0.61
550	0.99	0.89	1.32	0.65
650	0.94	0.92	1.34	0.75
750	1.02	0.93	1.23	0.78
850	1.04	0.91	1.33	0.79

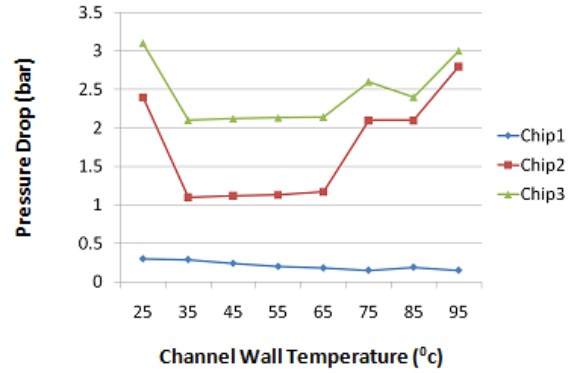


Figure 6. The pressure drop and channel wall temperature.

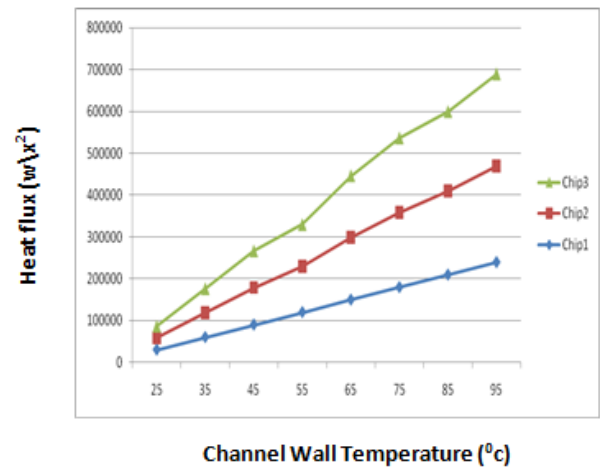


Figure 7. The heat flux and channel wall Temperature.

Table 5

pressure Drop	Chip1	Chip2	Chip3
25	0.3	2.4	3.1
35	0.29	1.1	2.1
45	0.24	1.12	2.12
55	0.2	1.13	2.13
65	0.18	1.17	2.14
75	0.15	2.1	2.6
85	0.19	2.1	2.4
95	0.15	2.8	3

Table 6

Temp	Chip1	Chip2	Chip3
25	30000	29000	28000
35	60000	59000	58000
45	90000	89000	88000
55	120000	110000	100000
65	150000	149000	148000
75	180000	179000	178000
85	210000	200000	190000
95	240000	230000	220000

Table 7

f	Re
5	25
10	5
15	4
20	4
25	4
30	3
35	3
40	3

V-shape Micro channel

For incompressible, fully-developed laminar flow, the friction factor can be expressed in terms of the two experimentally obtained parameters – pressure drop and mass flow rate.

$$f_{exp} = \frac{D_h}{L} \left(\frac{2\Delta P_{exp}}{\rho V_{av}^2} - \sum K_L \right) \quad \text{-----(V)}$$

where KL is the friction factor for the minor loss. For the comparison of values of f vs. Re as shown in Fig. 8, the differences between the results obtained from numerical simulation and those from traditional correlation are within 2.5% of each other, within 6% between the numerical simulations and the experimental data, and with the f vs. Re values obtained from the experimental data and those obtained from the numerical simulations approaching a fixed value which is slightly lower than the value of 53.3 predicted by the traditional

Wu and Cheng [22] proposed a correlation for the V-shaped microchannels ($W_b/W_t = 0$) for fluid at low Reynolds numbers as follows.

$$Nu = 6.7 Re^{0.946} Pr^{0.488} \left(1 - \frac{W_b}{W_t} \right)^{3.547} \left(\frac{W_t}{H} \right)^{3.577} \left(\frac{\epsilon}{D_h} \right)^{0.041} \left(\frac{D_h}{L} \right)^{1.369}, Re < 100 \quad \text{-----(VI)}$$

where W_b and W_t are the bottom and the top width of microchannel, respectively. And ϵ is the surface roughness.

Referring Wu and Cheng [23], Chu [3] proposed an empirical correlation, based on experimentally obtained data from four sets of triangular microchannel test specimens (with different channel widths) under low Reynolds number conditions ($Re < 50$).

$$Nu = 6.7 Re^{0.946} Pr^{0.488} \left(1 - \frac{W_b}{W_t} \right)^{3.547} \left(\frac{W_t}{H} \right)^{3.577} \left(\frac{\epsilon}{D_h} \right)^{0.041} \left(\frac{D_h}{L} \right)^{1.369}, Re < 100 \quad \text{-----(VI)}$$

Generally speaking, the trends of the predicted results obtained from the correlation specified by Eq. (VII) are in agreement, as shown in Fig. 9, while the widths of the micro channels have an obvious impact on the behavior of the development of the Nusselt numbers for the micro channels under study. It is noted that the magnitude of the Nusselt number increases at a slower rate as the Reynolds number becomes larger than 20.

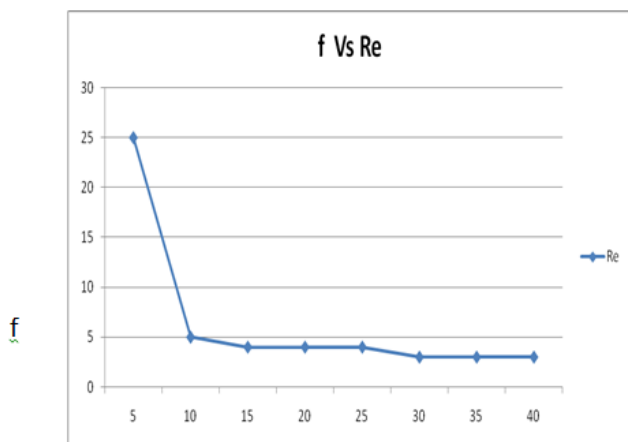


Figure 8. Comparison between f and Re for theoretical values, predicted values, and experimental data

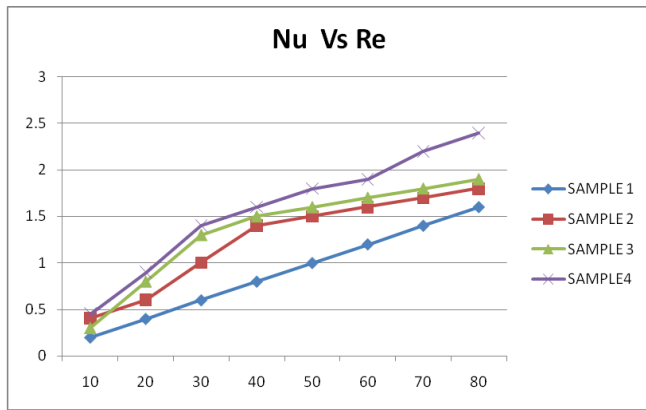


Figure 9. Comparison between Nu and. Re among empirical correlation and experimental data.

Table 9

Nu	SAMPLE1 1	SAMPLE2 2	SAMPLE3 3	SAMPLE4
10	0.2	0.4	0.3	0.45
20	0.4	0.6	0.8	0.9
30	0.6	1	1.3	1.4
40	0.8	1.4	1.5	1.6
50	1	1.5	1.6	1.8
60	1.2	1.6	1.7	1.9
70	1.4	1.7	1.8	2.2
80	1.6	1.8	1.9	2.4

It is also noted that high temperature gradients at the inlet and exit were observed from the temperature distributions of micro channels for all sets of the test specimens. In addition, the Nusselt numbers increase as the Reynolds number increases, as shown in Fig.9. For the range of the Reynolds number being tested ($Re > 50$), the average discrepancy of the values calculated from the correlation of Nu obtained in [3] and those obtained from the experimental data is within 19%; the difference is judged to be in fair agreement.

III. RESULTS AND DISCUSSION

The experiments are conducted for various channel geometries under different flows specially V-shape microchannel. Additionally, the flow visualization is used to describe the experimental results. Further, the uncertainties involved in the measurements were

analyzed and evaluated [19] and [21] which are given in Table 2.

To analyze the friction factor, the specifications of the sink are listed in Table 1. Chip 1–4 are prepared for fluid flow experiment. Figure 4 shows the relations between the friction factor and the Reynolds number. This denotes to be the laminar flow and the friction factor is decreasing with the power of Reynolds number. The computed value of f_{exp}/f_{thy} ranged from 0.8 to 1.4 is shown in Figure5, which matches the range of 1.0–1.6 by Mohiuddin-Mala [7].

Table1 shows the different microchannel geometries are selected for the heat transfer experiment.

The results are shown in Figure 6 and 7. In Figure 6, it is observed that the phenomenon of decreasing wall temperature during phase change is the same as Peng and Wang [12].

Figure 7, shows the relation between the inlet/outlet pressure drop and the wall temperature.

It is observed to have two sections, the single phase section and the phase transformation section.

In the single-phase section, the pressure drop between the inlet and outlet is obviously reduced with the wall temperature rises as the hydraulic diameter gets smaller. This is because of the viscosity coefficient of working fluid decreases with the temperature. When the channel wall temperature reaches the critical point for phase change, the fluid rapidly absorbs the accumulated energy on the channel for the violent nucleate boiling. Therefore, the tiny bubbles are formulated to sharply increase the pressure drop. After the severe nucleate boiling, the wall temperature greatly decreases and boiling phenomenon decelerates and the inlet/outlet pressure drop diminishes. Finally, the wall temperature grows again and much severe nucleate boiling follows to continuously boost the pressure drop.

It is also observed with flow visualization that there exists the nucleate boiling at the channel inlet. This retards the fluid flow and the pressure drop is thus suddenly enlarged. From Figure 6, it is noted that the result for Chip 3 is different from others. The channel temperature hardly decreased from the phase change, the heat transfer coefficient barely reduced from the high channel wall temperature, and the inlet/outlet pressure drop did not rapidly diminish from the severe nucleate boiling.

Therefore, it is found that the nucleate boiling occurs between Chip1 and Chip3. With this viewpoint, the critical bubble size of methanol is recognized to be in between 56–85 μm .

IV. CONCLUSIONS AND FUTURE WORK

Experimental tests and theoretical analyses are conducted to investigate the characteristics of fluid flow and heat transfer in micro-channel heat sink in this work. Methanol is used as the working fluid and flow through micro-channels with different hydraulic diameters ranging from 57–267 μm in the experiments we examined the experimental results of flow characteristics & check behavior of the laminar regime when $Re = 50\text{--}850$, the phenomena of transition exist or not.

This work is the experimentally studies the characteristics on both fluid flow and heat transfer of methanol in the (100) silicon micro-channel heat sink. This study would surely contribute a valuable approach to the micro cooling technology for solving the heat dissipation of precision and compact electronic components. The potential of developing combined V-shaped wavy lower plate with methanol as cooling using various particle volume fractions and base fluids in enhancing the heat transfer, the following finding can be drawn:

1. Micro channel heat sinks dissipate large amounts of heat with relatively little surface temperature rise.

2. As Reynolds number increases; the heat transfer coefficient, pressure drop and pumping power increases while thermal resistance and friction factor decreases.
3. To enhance the heat transfer in micro channel heat sink, it is necessary to study simultaneous effects of various parameters like size of channel, shape of channel, fluid properties, Reynolds number, friction factor, pressure drop, pumping power etc.
4. In the micro channel, the local heat flux q'' varies with the channel size, cross section of channel, shape of channel, fluid properties and the fluid flow arrangement.
5. It is found that the experimentally determined Nusselt number in micro channels is lower than that predicted by the theoretical analysis.
6. This study surely contributes a valuable approach to the micro cooling technology for solving the heat dissipation of precision and compact electronic components. Future researches with the in-situ temperature measurement in the micro channels to elaborate the results of this study are fully encouraged.

V. ACKNOWLEDGEMENT

The authors thank the honourable Vice chancellor of IFTM University, Moradabad for providing the necessary facilities and permission to carry out this research work. The authors also wish to acknowledge the research group of Physics Lab, School of Sciences, IFTM University for their constant help to complete this work.

NOMENCLATURE

L: overall channel length (m)

W: channel width (m)

D_h: hydraulic diameter of the microchannel (m)

ΔP : pressure drop between inlet and outlet (pa)

ρ_f : density of working fluid (kg/m³)

V_f: velocity of working fluid (m/s)

ΔP_{loss} : pressure loss between inlet and outlet (pa)

fthy: theoretical friction factor
 fexp: experimental friction factor
 I: current delivered from the power supply (Amp)
 V: voltage delivered from the power supply (volt)
 gc: unit change factor (1.0 kg m/N s²)
 K: pressure loss coefficient
 q": heat flux (W/m²)
 γ: mended factor
 Nu: Nusselt number
 Re: Reynolds number
 Pr : Prandtl number
 Wb : Bottom width of trapezoidal microchannels
 Wt :Top width of trapezoidal microchannels
 H : Microchannel height, m
 ε Surface roughness, m
 K_L: Friction factor for minor loss
 ρ: Density, kg m⁻³

VI. REFERENCES

- [1]. Tuckerman, D. B. and Pease, R. F. W., "High-Performance Heat Sinking for VLSI," *IEEE Electronic Device Letters*, Vol. EDL-2, pp. 126–129 (1981).
- [2]. Zhimin, W. and Kok-Fah, C., "The Optimum Thermal Design of Microchannel Heat Sinks," *IEEE/CPMT Electronic Packaging Technology Conference*, pp. 123–129 (1997).
- [3]. Yang, W. J. and Zhang, N. L., "Micro- and Nano-scale Heat Transfer Phenomena Research Trends," *Transport Science and Technology*, pp. 1–15 (1992).
- [4]. Peterson, G. P. and Ortega, A., "Thermal Control of Electronic Equipment and Devices," *Advances in Heat Transfer*, Vol. 17, pp. 181–314 (1990).
- [5]. Pfahler, J., Harley, J., Bau, H. H. and Zemel, J., "Liquid Transport in Micron and Submicron Channels," *J. Sensors Actors A*, Vol. 21–23, pp. 431–434 (1990).
- [6]. Choi, S. B., Barron, R. F. and Warrington, R. O. "Liquid Flow and Heat Transfer in Microtubes," *ASME Micromechanical Sensors, Actuators and Systems*, Vol. 32, pp. 123–128 (1991).
- [7]. Mala, G. M. and Li, D., "Flow Characteristics of Water in Micro Tubes," *Int. J. Heat and Fluid Flow*, Vol. 20, pp. 142–148 (1999).
- [8]. Weilin, Q., Mala, G. and Li, M. D., "Pressure-driven Water Flows in Trapezoidal Silicon Microchannels," *Int. J. Heat and Mass Transfer*, Vol. 43, pp. 353–364 (1999).
- [9]. Peng, X. F., Peterson, G. P. and Wang, B. X., "Frictional Flow Characteristics of Water Flowing through Rectangular Microchannels," *Experimental Heat Transfer*, Vol. 7, pp. 249–264 (1994).
- [10]. Peng, X. F. and Wang, B. X., "Forced Convection and Flow Boiling Heat Transfer for Liquid Flowing through Microchannels," *Int. J. Heat Mass Transfer*, Vol. 36, pp. 3421–3427 (1993).
- [11]. Wang, B. X. and Peng, X. F., "Experimental Investigation on Liquid Forced Convection Heat Transfer through Microchannels," *Int. J. Heat Mass Transfer*, Vol. 37 Suppl. 1, pp. 73–82 (1994).
- [12]. Peng, X. F., Peterson, G. P. and Wang, B. X., "Heat Transfer Characteristics of Water Flowing through Microchannels," *Experimental Heat Transfer*, Vol. 7, pp. 265–283 (1994).
- [13]. Peng, X. F., Wang, B. X., Peterson, G. P. and Ma, H. B., "Experimental Investigation of Heat Transfer in Flat Plates with Rectangular Microchannels," *Int. J. Heat and Mass Transfer*, Vol. 38, pp. 127–137 (1995).
- [14]. Peng, X. F. and Peterson, G. P. "The Effect of Thermofluid and Geometrical Parameters on Convection of Liquids through Rectangular Microchannels," *Int. J. Heat and Mass Transfer*, Vol. 38, pp. 755–758 (1995).
- [15]. Peng, X. F. and Peterson, G. P., "Convective Heat Transfer and Flow Friction for Water Flow in Microchannel Structure," *Int. J. Heat and Mass Transfer*, Vol. 39, pp. 2599–2608 (1996).

- [16]. Peng, X. F., Hu, H. Y. and Wang, B. X., "Boiling Nucleation during Liquid Flow in Microchannels," *Int. J. Heat and Mass Transfer*, Vol. 41, pp. 101–106 (1998).
- [17]. Peng, X. F., Hu, H. Y. and Wang, B. X., "Flow Boiling through V-shape Microchannels," *Experimental Heat Transfer*, Vol. 11, pp. 87–90 (1998).
- [18]. Peng, X. F. and Wang, B. X., "Boiling Characteristics in Microchannels/Microstructures," *The 11th Int. Symposium on Transport Phenomena, ISTP-11*, pp. 485–491 (1998).
- [19]. Jiang, L., Wong, M. and Zohar, Y., "Phase Change in Microchannel Heat Sinks with Integrated Temperature Sensors," *J. of Microelectromechanical System*, Vol. 8, pp. 358–365 (1999).
- [20]. Naphon P. Heat transfer characteristics and pressure drop in channel with Corrugated upper and lower plates. *Energy Converse Manag* 2007;48:1516–24.
- [21]. Naphon P, Kornkumjayrit K. Numerical analysis on the fluid flow and heat transfer in the channel with V-shaped wavy lower plate. *Intl Commun Heat Mass Transf* 2008;35:839–43.
- [22]. H. Y. Wu and P. Cheng, "An experimental study of convective heat transfer in silicon microchannels with different surface conditions," *International Journal of Heat and Mass Transfer*, Vol. 46, pp. 2547-2556, 2003.
- [23]. H. Y. Wu and P. Cheng, "Friction factors in smooth trapezoidal silicon microchannels with different aspect ratios," *International Journal of Heat and Mass Transfer*, Vol. 46, pp. 2519-2525, 2003.
- [24]. Yu-Tang Chen et al.: "Experimental Investigation of Fluid Flow and Heat Transfer in Microchannels" *Tamkang Journal of Science and Engineering*, Vol. 7, No. 1, pp. 11–16 (2004).
- [25]. A.M. Abedetal. Enhance heat transfer in the channel with V-shaped wavy Lower plate using liquid nano fluids /Case Studies in Thermal Engineering 5 (2015) 13–23.
- [26]. Jyh-tong Teng, Jiann-Cherng Chu, Chao Liu, Tingting Xu, Yih-Fu Lien, Jin-Hung Cheng, Suyi Huang, Shiping Jin, Thanhtrung Dang, Chunping Zhang, Xiangfei Yu, Ming-Tsang Lee, and Ralph Greif (2012). *Fluid Dynamics in Microchannels, Fluid Dynamics, Computational Modeling and Applications*, Dr. L. Hector Juarez (Ed.), ISBN: 978-953-51-0052-2,